

Experimental and Numerical Investigations of Three-Dimensional Dam-Break Flows

Azim Shirdeli^{1,*}, Vahid Naderkhanloo², Ali Samadi Rahim²

¹ Water Engineering Department, Zanjan University, Iran

² Water Engineering Department, Tarbiat Modares University, Iran

Abstract: The numerical model can be used to predict flood wave propagation and provide the information about the flood properties. The purpose of this paper is to presents simulation of dam-break problem by three dimensional model of Mike3 Flow Model FM. The model is verified with laboratory experimental test case on a frictionless horizontal bottom for water surface elevation in five benchmark points. A good agreement between experimental data and simulation results is observed. The computed arrival time of the flood wave front and the maximum flow depths at various observation points matched well with the measurements on physical model. Also, turbulence modeling does not affect the velocity profile in the upstream reservoir, but has significant influence on the prediction of downstream velocity; the velocity magnitude at a specific location changes with time, but the shape of the velocity profiles remains similar. Therefore, the Mike3 model can correctly account for complex dam-break flows and giving a satisfactory prediction of the major characteristics such as water depth, flood extent, flood wave arrival time and velocity profiles. The results indicate that this model can be applied for simulation of dam-break problem in real life cases.

[Azim Shirdeli, Vahid Naderkhanloo, Ali Samadi Rahi. **Experimental and Numerical Investigations of Three-Dimensional Dam-Break Flows**. *Stem Cell* 2019;10(3):34-43]. ISSN: 1945-4570 (print); ISSN: 1945-4732 (online). <http://www.sciencepub.net/stem>. 7. doi:[10.7537/marsscj100319.07](https://doi.org/10.7537/marsscj100319.07).

Keywords: Dam-Break Flows, Flood Simulations, Mike3 Flow Model FM, Three-Dimensional Model.

1. Introduction

A dam break is the partial or catastrophic failure of a dam which leads to an uncontrolled release of water (Fread, 1993). Flood inundation due to dam and levee breach often cause serious loss of life and property. Dam failures are often caused by structural deficiencies, such as poor initial design or construction, or due to lack of maintenance and repairs (Bell *et al.*, 1992). In order to assess the consequences of a dam failure event, simulation of the resulting flood is of great importance. The spatial and temporal variations of water depths and velocities during a dam break event are important parameters for hydraulic engineers in order to prepare emergency action plans in a risk based framework. Accurate estimates of flow depths and flow velocity are key factors for emergency planning for potential dam-break floods. The numerical model can be used to predict flood wave propagation and provide the information about the flood extent, flood wave arrival time and water depth etc. Therefore, it is a useful tool for establishing flood control and dam operating strategies as well as developing evacuation plans and warning systems for the areas having potential flood risk.

In recent years, there has been a substantial research emphasis on the development of numerical models to simulate dam-break flows. A number of numerical models of dam-break flow have been developed by solving 1D and 2D depth-averaged continuity and momentum equations of open-channel

flow commonly known as the Saint-Venant or the shallow water equations. The shallow water equations have been solved numerically by the method of characteristics, finite element, finite difference, and the finite volume modeling techniques (e.g., Katopodes and Strelkoff, 1978; Akanbi and Katopodes, 1988; Fennema and Chaudhry, 1989, 1990; Elliot and Chaudhry, 1992; Alcrudo and Navarro, 1993; Fraccarollo and Toro, 1995; Alam and Bhuiyan, 1995; Jha *et al.*, 1995; Bradford and Sanders, 2005; Soares-Frazao and Zech, 2007). Other examples of successful representation of dam-break flows with the shallow water approach are: Xanthopoulos *et al.*, 1976; Hromadka *et al.*, 1985; Aricò *et al.*, 2007. Brufau *et al.* (2002) developed a numerical model for dam-break flows and resolved the wetting and drying of irregular terrain to a good extent. Brufau *et al.* (2004) developed a 2D numerical model for dam-break flows and achieved a zero mass error by modifying the wetting-drying condition which included the normal velocity to the cell edges.

The three-dimensional numerical simulations performed by Manciola *et al.* (1994) and De Maio *et al.* (2004) show that the SW approach may underestimate the wave front celerity and may fail in correctly reproducing water depth profiles. Several three-dimensional CFD models, based on the complete set of the Navier Stokes equations, have been already applied to typical hydraulic engineering cases, as flow over weirs, landslide generated waves, through bridge piers and dam breaks (G'omez-

Gesteira and Dalrymple, 2004; Nagata, 2005; Quecedo *et al.*, 2005; Liang *et al.*, 2007; Mohammadi, 2008). Therewith, Navier–Stokes equations solvers along with surface tracking algorithms have been used by a few researchers to study 2D dam-break flows (e.g., Yue *et al.*, 2003; Biscarini *et al.*, 2010).

In this present research, we compare the experimental data with the modeling results deriving from Mike3 Flow Model FM numerical model. In all the experiments, effects of friction are inconsiderable. Whereas, even if frictionless simulations are not realistic, the present paper is focused on highlighting the performances of hydraulic numerical methods on typical simplified test case. Thus, the selection of an appropriate model to correctly simulate dam-break flood routing is necessary. Traditionally, one and two-dimensional models have been used to model dam break flooding, but these models are limited in their ability to capture the flood spatial extent, in terms of flow depth and velocity and timing of flood arrival and recession, with any degree of detail. Therefore, the 3D numerical model of Mike3 has been chosen for simulation of dam-break phenomena. The present work has the following main objectives: (1) to simulate the experiments using Mike3 model; (2) to collect data on the spatiotemporal evolution of water surface and velocity in the downstream flooded area and upstream reservoir from a 3D numerical method; and (3) to compare experimental and simulation results.

2. Materials and Methods

2.1 Numerical modeling

Mike3 is a commercial computational fluid dynamics package that used to simulate the dam-break experiments. This model is a comprehensive modeling

system for three-dimensional water modeling developed by DHI. The modeling system has been developed for complex applications within oceanographic, coastal and estuarine environments. However, being a general modeling system for 3D free surface flows it may also be applied for studies of inland surface waters, e.g. overland flooding and lakes or reservoirs. The modeling system is based on the numerical solution of the three-dimensional incompressible Reynolds averaged Navier-Stokes equation subject to the assumptions of Boussinesq and of hydrostatic pressure. The spatial discretisation of the governing equations is performed using a cell-centred finite volume method. In the horizontal plane an unstructured grid is used while a structured mesh is used in the vertical domain (Fig. 1). The free surface is taken into account using a sigma-coordinate transformation approach or using a combination of a sigma and z-level coordinate system.

When high free surface gradients exist, such as those at the failure site during the first instants, or when physical obstacles or steep changes on the bed slope are encountered by the flood wave, this assumption is no longer valid. Therefore, non-simplified models are needed to accurately solve the three-dimensional structure of the flow in these areas (Fraccarollo and Toro, 1995; Mohapatra *et al.*, 1999). The three-dimensional multiphase approach proposed here is based on the numerical resolution of the incompressible RANS equations.

2.1.1 Governing equations

The filtered or Reynolds-averaged conservation equations for mass and momentum using Cartesian coordinates for an incompressible fluid has been expressed underneath. The local continuity equation is written as:

$$\frac{\partial u}{\partial x} + \frac{\partial v}{\partial y} + \frac{\partial w}{\partial z} = S \quad (1)$$

and the momentum equation for the x-component is:

$$\begin{aligned} \frac{\partial u}{\partial t} + \frac{\partial u^2}{\partial x} + \frac{\partial uv}{\partial y} + \frac{\partial uw}{\partial z} = & fv - g \frac{\partial \eta}{\partial x} - \frac{1}{\rho_o} \frac{\partial P_a}{\partial x} - \frac{g}{\rho} \int_z^\eta \frac{\partial \rho}{\partial x} dz \\ - \frac{1}{\rho_o h} \left(\frac{\partial s_{xx}}{\partial x} + \frac{\partial s_{xy}}{\partial y} \right) + F_u + \frac{\partial}{\partial z} \left(v_t \frac{\partial u}{\partial z} \right) + u_s S \end{aligned} \quad (2)$$

where t is the time; x , y and z are the Cartesian coordinates; η is the surface elevation; $h = \eta + d$ is the total water depth; d is the still water depth; u , v and w are the velocity components in the x , y and z direction;

$f = 2\Omega \sin \phi$ is Coriolis parameter (Ω is the angular rate of revolution and ϕ the geographic latitude); g is the gravitational acceleration; ρ is the density of water; s_{xx} and s_{xy} are components of the

radiation stress tensor; ν_t is the vertical turbulent (or eddy) viscosity; P_a is the atmospheric pressure; ρ_o is the reference density of water. S is the magnitude of the discharge due to point sources and u_s is velocity by which the water is discharged into the ambient water and F_u is the horizontal stress of flow term.

2.1.2 Turbulence modeling

The turbulence is modeled using an eddy viscosity concept. The eddy viscosity is often described separately for the vertical and the horizontal transport. In many numerical simulations the small-scale turbulence can not be resolved with the chosen spatial resolution. This kind of turbulence can be approximated using sub-grid scale models.

a) Vertical eddy viscosity

The eddy viscosity derived from the log-law is calculated by:

$$\nu_t = U_\tau h \left(c_1 \frac{z+d}{h} + c_2 \left(\frac{z+d}{h} \right)^2 \right) \quad (3)$$

where $U_\tau = \max(U_{\tau_s}, U_{\tau_b})$; U_{τ_s} and U_{τ_b} are the friction velocities associated with the surface and bottom stresses; $c_1 = 0.41$ and $c_2 = -0.41$ give the standard parabolic profile.

b) Horizontal eddy viscosity

In many applications a constant eddy viscosity can be used for the horizontal eddy viscosity. Alternatively, Smagorinsky (1963) proposed to express sub-grid scale transports by an effective eddy viscosity related to a characteristic length scale. The sub-grid scale eddy viscosity is given by:

$$A = c_s^2 l^2 \sqrt{2S_{ij}S_{ij}}$$

$$S_{ij} = \frac{1}{2} \left(\frac{\partial u_i}{\partial x_j} + \frac{\partial u_j}{\partial x_i} \right)$$

where c_s is a constant rate of Smagorinsky coefficient; l is a characteristic length; S_{ij} is deformation rate.

2.2 Validation of model

In order to test the capability of the employed numerical model of performing transient simulations, a dam-break in a reservoir has been modeled and the numerical results compared to the experimental data. The validation of the proposed model is performed by simulating the laboratory experiment case of flood wave propagation on a horizontal bottom due to partial dam break reported by Fraccarollo and Toro

(1995). The schematic view of the experimental set is shown in Fig. 2. The reservoir is 1 m long and 2 m wide and the floodplain is 3 m long and 2 m wide. The breach is 0.4 m wide and located at the middle of the dam. In the selected case, the initial water depth in the reservoir is 0.6 m. The floodplain is initially dry. The bottom of the reservoir and floodplain is horizontal. The location of 5 measuring gauges is indicated in Fig. 2 and their coordinates are listed in Table 1. Also, the dam breaches instantaneously.

2.3 Simulations setup

The test consists of simulating the submersion wave due to the partial collapse of a dam. The experimental case is represented on a triangular mesh with 6897 nodes and maximum area element 0.001 m². At the beginning of the simulation the water surface levels is set in 0.6 m for the upstream region and dry for the downstream and the unsteady flow is generated by the instantaneous collapse of the dam. The bed is horizontal and the wall friction and ground resistance to the motion is neglected. Also, surface tension effects between wall and water-air interface are neglected. A null flow rate in the inlet section is set as the initial condition. The boundary conditions are no flow type at the location of the reservoir and along the floodplain walls. The simulation carried out using a time step of 0.02 s, with a Courant number never exceeding 0.8.

3. Results and Discussion

As the dam collapse instantaneously, a surge wave propagates in the downstream flood plain while the rarefaction wave propagates towards boundaries causing the water level to drop in the reservoir. The observed water depth at 5 measuring stations (experimental case) is compared with the numerical simulations and the results are indicated in Fig. 3. Notice to Fig. 3, the overall agreement between the measured and the computed results is reasonable. After the sudden opening of the gate, a surge is formed and propagates over the floodplain. Simultaneously, a strong depression wave occurs in the reservoir and causes the water surface near the gate to descend drastically. Because of the effects of boundary reflection, water surface in the reservoir oscillates significantly in the initial stage. All these details are well reproduced by the numerical model. The stations -5A and C are equidistant from the center of the breach; thus the depth hydrographs at these locations are almost similar. The simulated results of flood depth at these two locations are in good agreement with the experiments. Station 4 is located at the left end of the dam where the streamlines are curved. The model reasonably estimated the flow depth in the initial phase of the dam-break wave propagation. At measuring station 0, which is in the

center of the breach, the model correctly evaluated the flow depth and simulated results accordance to experiments. The flow depth at a downstream station, 8A, is reproduced up to a reasonable accuracy. Overall, the performance of the model in simulating a 3D ideal dam-break can be termed as good.

Computed flood wave profiles (or consist of water depth) and velocity magnitude at different times for upstream reservoir and flooded downstream at central line of the model are shown in Figs. 4 (a-e). It should be noted that in Figs. 4 (a-e) the location of the dam is $x = 1 \text{ m}$. The velocity magnitude was relatively small at the far upstream location as compared with that near the dam. At $t = 1 \text{ s}$, the velocity magnitude was over 3.5 m/s at location $x = 1.2 \text{ m}$, but had a much smaller value of 2.1 m/s at $t = 4 \text{ s}$. At location $x = 1.2 \text{ m}$, the velocity increased to its maximum value at $t = 1 \text{ s}$, and then started to decrease as the reservoir water level dropped. Generally, the flood wave moves with speed and more power at $t = 1 \text{ s}$, because the water level in the reservoir is still high, so the potential energy is converted to kinetic energy. But by decreasing water level in the reservoir reduced flood velocity to the lowest level, as in Fig. 4e ($t = 4 \text{ s}$) appears. Due to the instantaneous collapse of the dam, the water surface (And consequently the velocity vectors) will have an intensive curvature, whereas upstream of the dam in distance of approximately 0.3 m ($x = 0.7 \text{ m}$) come about highest hillock on the water surface. Water surface curvature in the upstream of the dam reached its maximum at time of 1 s and drops the water level of the reservoir reduced water surface hillock. It is noted which the maximum curvature on the water surface occurred in the initial times and reaches maximum rate at the time of 1 s .

Figs. 5, 6 and 7 show value of velocity and flow patterns simulated for the whole upstream reservoir and downstream floodplain in the various times. Fig. 5 indicates flow pattern and velocity values at $t = 1 \text{ s}$. As can be observed in the sides of the dam has occurred maximum velocity. Also, the flow pattern represents the maximum curvature at this region, because the flow feels existence of the dam on the path as well. Moreover, can be estimated amount of the flood wave headway at $t = 1 \text{ s}$ from Fig. 5. Flood wave is located at a distance of 1.4 m from downstream of the dam. However, this can be received from Fig. 4b. Fig. 6 provides the flow pattern

at $t = 2 \text{ s}$. This Figure may be perceived that flood wave traveled throughout of the floodplain approximately in 2 s . Therefore, can be concluded dam-break phenomena will be progress rapidly in downstream area. Flow pattern at $t = 10 \text{ s}$ are shown in Fig. 7. Due to great reduction in reservoir water level, curvature of stream lines reached minimum rate at this time, as well as the flow velocity is the lowest value. It should be noted that the decreasing height of water in the reservoir, the location of maximum flow velocity recedes from downstream of the dam, so that at $t = 10 \text{ s}$ the maximum velocity occurs approximate location in $x = 0.5 \text{ m}$. Maximum value of velocity in the downstream floodplain occurs at $t = 1 \text{ s}$ and over time and reducing the reservoir water surface level; the flow velocity is decreased in this region. An important issue in the flow pattern is symmetry in the flow pattern at all times. It is well-understood in Figs. 5 to 7.

4. Conclusion

The present paper addresses a relevant problem in hydraulic engineering: the selection of an appropriate model to undertake dam break flood routing. The capability of the Mike3 model to correctly simulate transient free surface simulations has been validated by comparing numerical solution with the experimental results of a partial dam-break. The comparison between simulated and experimental results, clearly shows that the three-dimensional model has the capability to represent the unsteady flow behavior quite well in the whole observation period, while some slightly differences between experimental data and numerical results are observed. Furthermore, the three-dimensional model may provide complete and detailed information on the physical quantities in space and time, which in turn give information on the potential flood evolution especially in terms of water depth, free surface profile, flow velocity, wave front dynamics etc. also over complicated terrain profiles and frequent discontinuities. Time evolution of velocity profiles in the upstream reservoir and the flooded downstream area and change of the water surface level was obtained using 3D model. Numerical simulation with the Navier–Stokes turbulence model successfully predicted the variation of the velocity profiles with time and distance. It is demonstrated that the model is capable to predict real life flood wave propagations due to dam and levee breach.

Table 1. Location of observation points in experiment model (Fraccarollo and Toro, 1995)

| Stations | -5A | C | 4 | 0 | 8A |
|----------|------|------|------|------|------|
| x (m) | 0.18 | 0.48 | 1.00 | 1.00 | 1.72 |
| y (m) | 1.00 | 0.40 | 1.16 | 1.00 | 1.00 |

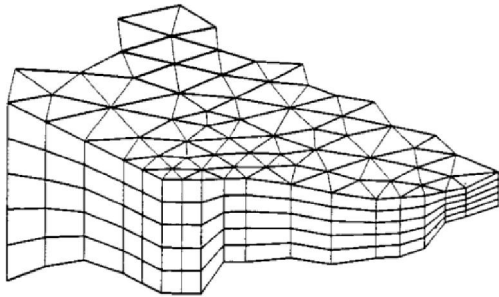


Fig. 1. Principle of meshing for the three-dimensional case

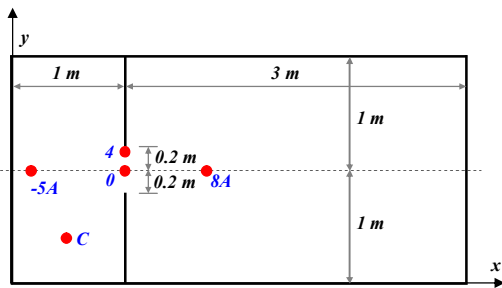


Fig. 2. Sketch of experiment set of Fraccarollo and Toro (1995) and location of the measuring points

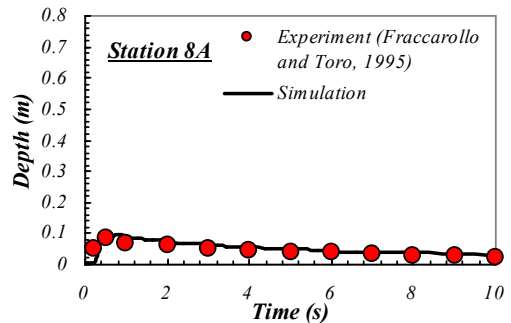
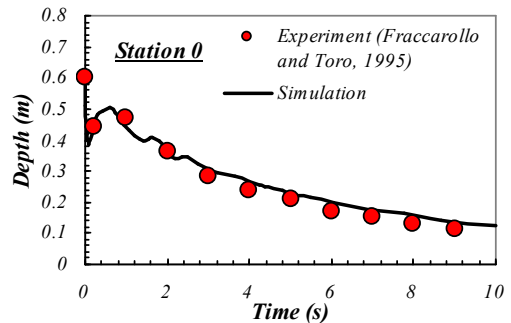
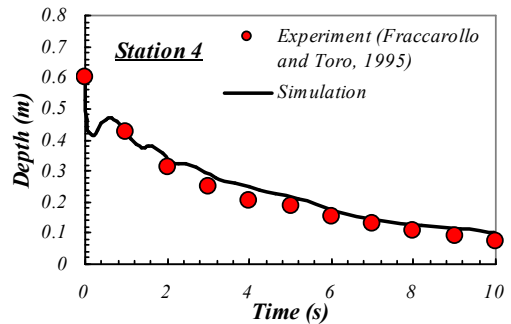
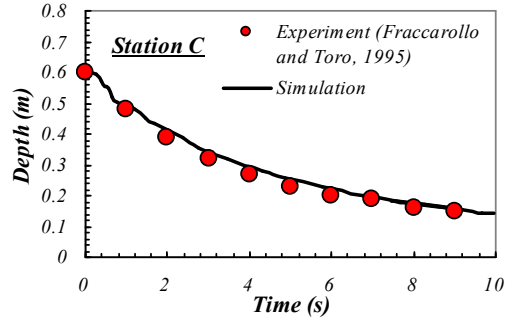
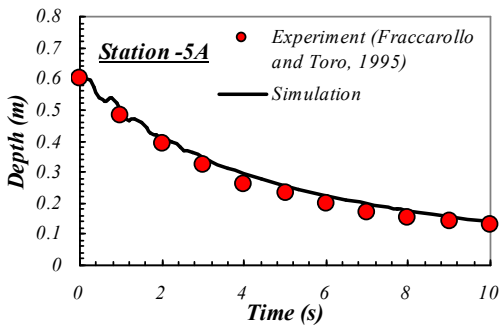


Fig. 3. Comparison of experiments results with numerical simulation for all measurement points

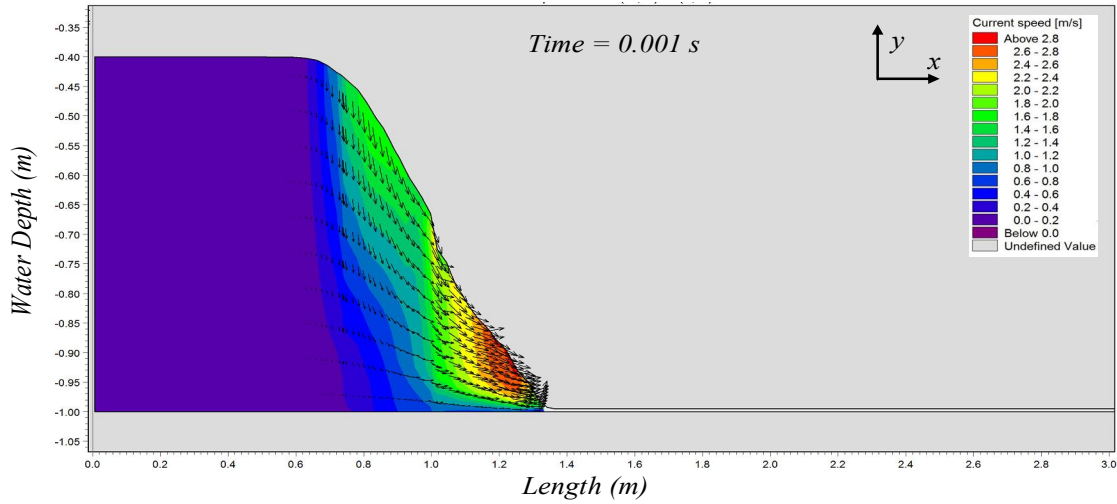


Fig. 4a. Flood wave profile and velocity magnitude at $t = 0.001$ s

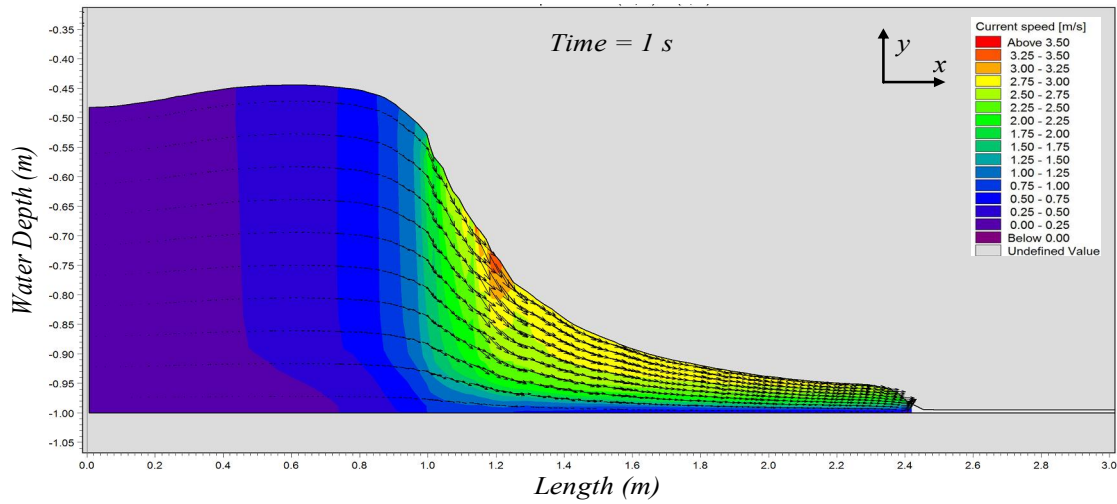


Fig. 4b. Flood wave profile and velocity magnitude at $t = 1$ s

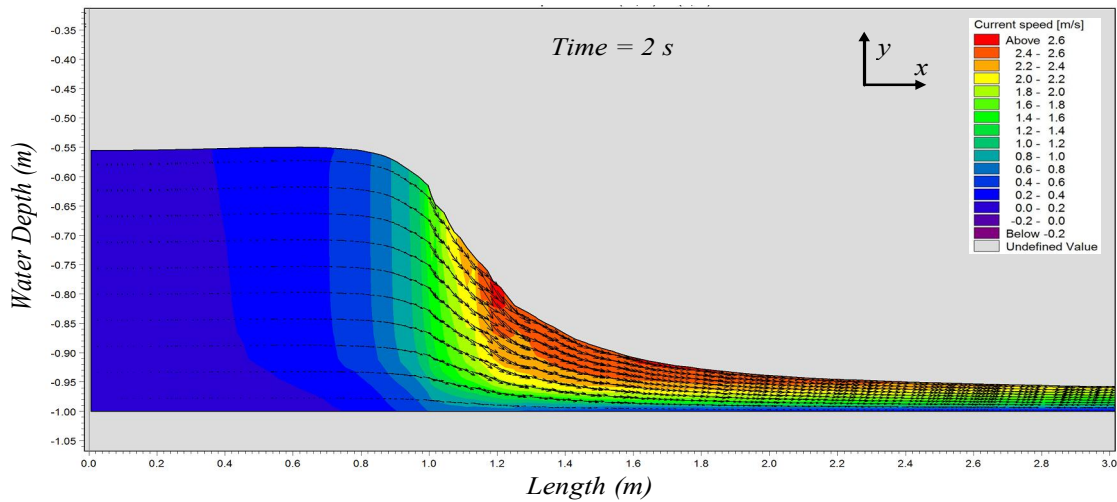


Fig. 4c. Flood wave profile and velocity magnitude at $t = 2$ s

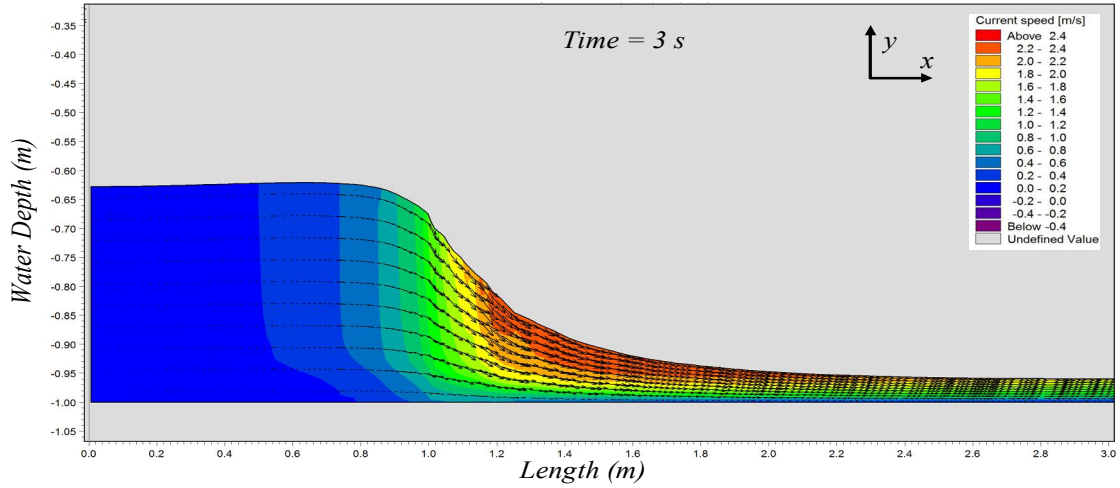


Fig. 4d. Flood wave profile and velocity magnitude at $t=3$ s

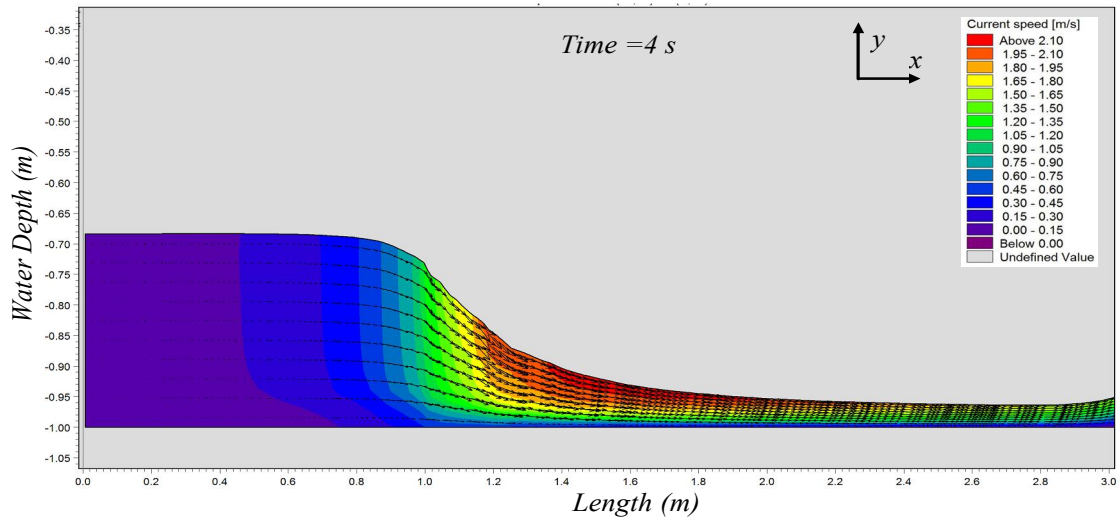


Fig. 4e. Flood wave profile and velocity magnitude at $t=4$ s

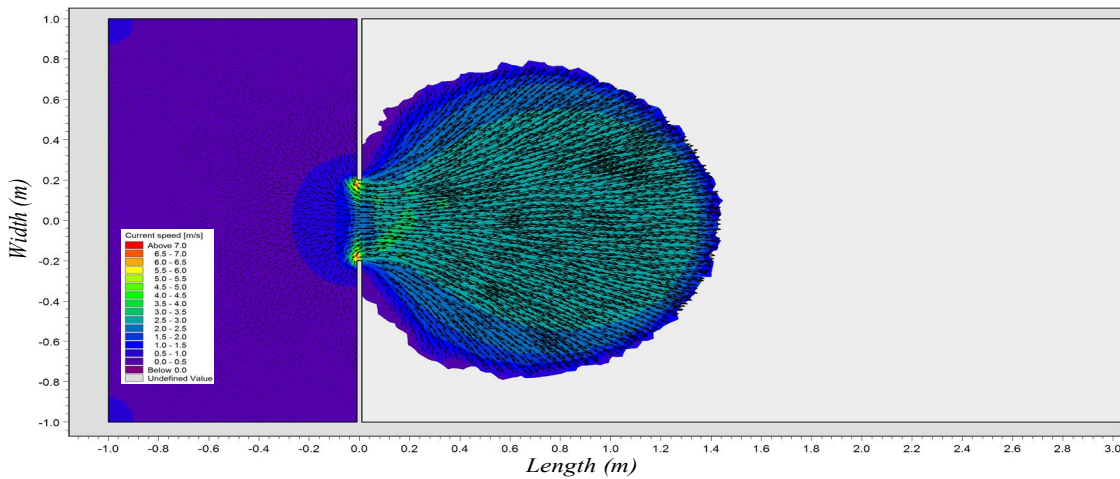
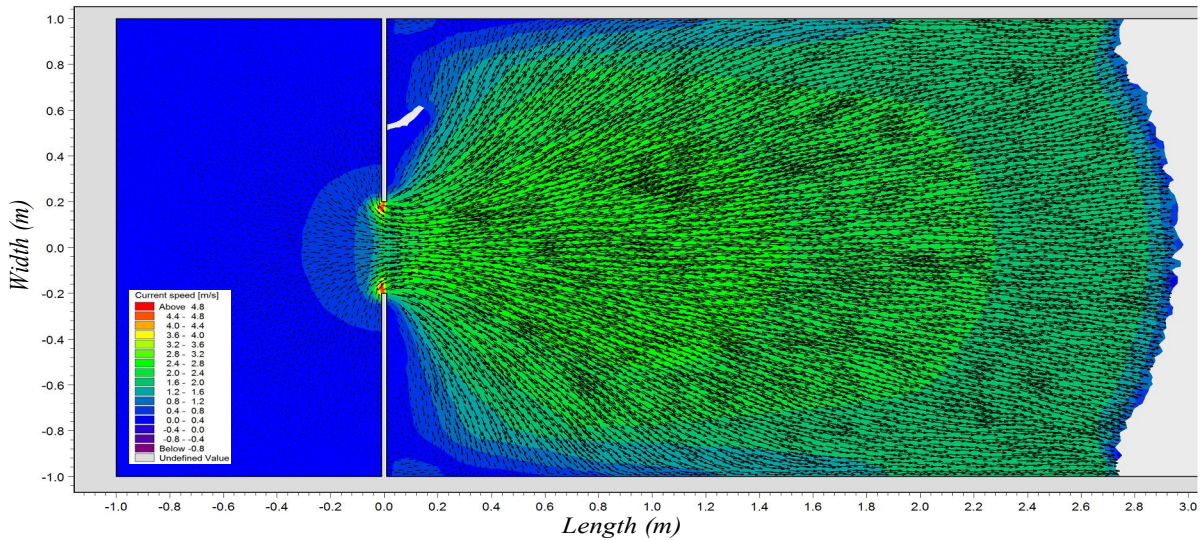
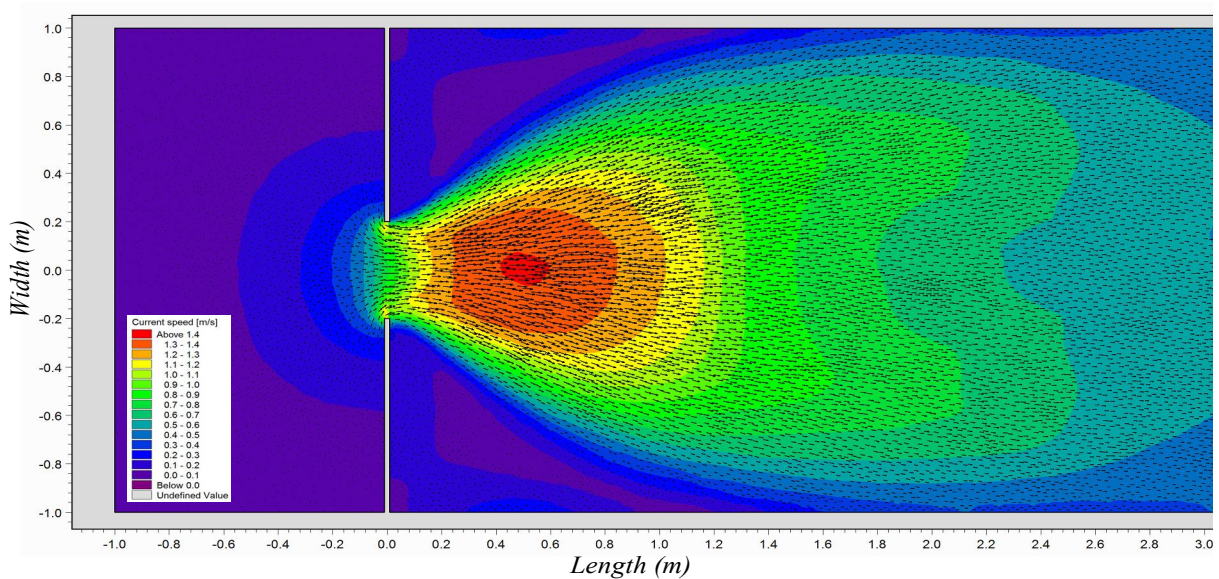


Fig. 5. Simulated flow pattern and velocity at $t=1$ s

Fig. 6. Simulated flow pattern and velocity at $t=2$ sFig. 7. Simulated flow pattern and velocity at $t=10$ s**Authors:**Azim Shirdeli^{1,*}, Vahid Naderkhanloo², Ali Samadi Rahim²¹ Water Engineering Department, Zanjan University, Iran² Water Engineering Department, Tarbiat Modares University, Iran**References**

1. Akanbi AA, Katopodes N. 1988. Model for flooding propagation on initially dry land. *J. Hydraul. Eng.*, 114, 689–706. [doi: 10.1061/\(ASCE\)0733-9429\(1988\)114:7\(689\)](https://doi.org/10.1061/(ASCE)0733-9429(1988)114:7(689)).
2. Alam MM, Bhuiyan MA. 1995. Collocation finite-element simulation of dam-break flows. *J. Hydraul. Eng.*, 121, 118-131.

- [doi:http://dx.doi.org/10.1061/\(ASCE\)0733-9429\(1995\)121:2\(118\)](http://dx.doi.org/10.1061/(ASCE)0733-9429(1995)121:2(118)).
3. Alcrudo F, Garcia-Navarro P. 1993. A high-resolution Godunov type scheme in finite volumes for the two-dimensional shallow water equations. *Int. Journ. Num. Methods in Fluids*, 16, 489–505. [doi:10.1002/flid.1650160604](http://dx.doi.org/10.1002/flid.1650160604).
 4. Aricò C, Nasello C, Tucciarelli T. 2007. A Marching in Space and Time (MAST) solver of the shallow water equations, Part II: the 2-D model. *Adv. Water Res.*, 30, 1253–1271. [doi:10.1016/j.advwatres.2006.11.003](http://dx.doi.org/10.1016/j.advwatres.2006.11.003).
 5. Bell S, Elliot R, Chaudhry MH. 1992. Experimental results of two-dimensional dam-break flows. *J. Hydraul. Res.*, 30, 225–252. [doi:10.1080/00221689209498936](http://dx.doi.org/10.1080/00221689209498936).
 6. Biscarini C, Francesco SD, Manicola P. 2010. CFD modeling approach for dam break flow studies. *Hydrol. Earth Syst. Sci.*, 14, 705–718. [doi:10.5194/hess-14-705-2010](http://dx.doi.org/10.5194/hess-14-705-2010).
 7. Bradford S, Sanders B. 2005. Performance of high-resolution, non-level bed, shallow water models. *J. Eng. Mech.*, 131, 1073–1081. [doi:http://dx.doi.org/10.1061/\(ASCE\)0733-9399\(2005\)131:10\(1073\)](http://dx.doi.org/10.1061/(ASCE)0733-9399(2005)131:10(1073)).
 8. Brufau P, Garcia-Navarro P, Vazquez-Cendon ME. 2004. Zero mass error using unsteady wetting–drying conditions in shallow flows over dry irregular topography. *Int J Numer Methods Fluids*, 45, 1047–82. [doi:10.1002/flid.729](http://dx.doi.org/10.1002/flid.729).
 9. Brufau P, Vazquez-Cendon ME, Garcia-Navarro P. 2002. A numerical model for flooding and drying of irregular domains. *Int J Numer Methods Fluids*, 39, 247–75. [doi:10.1002/flid.285](http://dx.doi.org/10.1002/flid.285).
 10. De Maio A, Savi F, Sclafani L. 2004. Three-dimensional Mathematical Simulation of Dam-break Flow. *Proceeding of IASTED conferences – Environmental Modeling and Simulation* ISBN: 0-88986-441-1 St. Thomas, US Virgin Island.
 11. Elliot R, Chaudhry M. 1992. A wave propagation model for two-dimensional dam-break flows. *J. Hydraul. Res.*, 30, 467–483. [doi:10.1080/00221689209498895](http://dx.doi.org/10.1080/00221689209498895).
 12. Fennema R, Chaudhry M. 1989. Implicit method for two-dimensional unsteady free-surface flows. *J. Hydraul. Res.*, 27, 331–332. [doi:10.1080/00221688909499167](http://dx.doi.org/10.1080/00221688909499167).
 13. Fennema RJ, Chaudhry MH. 1990. Explicit methods for two-dimensional transient free-surface flows. *JHE*, 116, 1013–1034. [doi:http://dx.doi.org/10.1061/\(ASCE\)0733-9429\(1990\)116:8\(1013\)](http://dx.doi.org/10.1061/(ASCE)0733-9429(1990)116:8(1013)).
 14. Fraccarollo L, Toro EF. 1995. Experimental and numerical assessment of the shallow water model for two-dimensional dam-break problems. *J. Hydr. Res.*, 33, 843–864. [doi:10.1080/00221689509498555](http://dx.doi.org/10.1080/00221689509498555)
 15. Fread DL. 1993. Flow Routing in *Handbook of Hydrology*. edited by Maidment DR, McGraw-Hill Inc., New York, USA, 902.
 16. G´omez-Gesteira M, Dalrymple RA. 2004. Using a three-dimensional smoothed particle hydrodynamics method for wave impact on a tall structure. *J. Waterway, Port, Coastal and Ocean Eng.*, 130, 63–69. [doi:http://dx.doi.org/10.1061/\(ASCE\)0733-950X\(2004\)130:2\(63\)](http://dx.doi.org/10.1061/(ASCE)0733-950X(2004)130:2(63)).
 17. Hromadka TV, Berenbrock CE, Freckleton JR, Guymon GL. 1985. A two-dimensional dam-break flood plain model. *Adv. Wat. Res.*, 8, 7–14 March. [doi:10.1016/0309-1708\(85\)90074-0](http://dx.doi.org/10.1016/0309-1708(85)90074-0).
 18. Jha AK, Akiyama J, Ura M. 1995. First- and second-order flux difference splitting schemes for dam-break problem. *J. Hydraul. Eng.*, 121, 877–892. [doi:10.1061/\(ASCE\)0733-9429\(1995\)121:12\(877\)](http://dx.doi.org/10.1061/(ASCE)0733-9429(1995)121:12(877)).
 19. Katopodes N, Strelkoff T. 1978. Computing two-dimensional dam-break flood waves. *J. Hydraul. Div.*, 104, 1269–1288.
 20. Liang D, Lin B, Falconer RA. 2007. Simulation of rapidly varying flow using an efficient TVD-MacCormack scheme. *Int. J. Numer. Meth. Fl.*, 53, 811–826. [doi:10.1002/flid.1305](http://dx.doi.org/10.1002/flid.1305).
 21. Manciola P, Mazzoni A, Savi F. 1994. Formation and Propagation of Steep Waves: An Investigative Experimental Interpretation. *Proceedings of the Specialty Conference Co-sponsored by ASCE-CNR/CNDCI-ENEL spa held in Milan, Italy, 29 June–1 July*.
 22. Mohammadi M. 2008. Boundary shear stress around bridge piers. *Am. J. Appl. Sci.*, 5, 1547–1551. [doi:http://dx.doi.org/10.1061/40569\(2001\)255](http://dx.doi.org/10.1061/40569(2001)255).
 23. Mohapatra PK, Eswaran V, Bhallamudi SM. 1999. Two-dimensional analysis of dam-break flow in vertical plane. *J. Hydr. Engng. ASCE*, 125, 183–192. [doi:http://dx.doi.org/10.1061/\(ASCE\)0733-9429\(1999\)125:2\(183\)](http://dx.doi.org/10.1061/(ASCE)0733-9429(1999)125:2(183)).
 24. Nagata N, Hosoda T, Nakato T, Muramoto Y. 2005. Three-Dimensional Numerical Model for Flow and Bed Deformation around River Hydraulic. *J. Hydraul. Eng.-ASCE*, 131, 1074–1087. [doi:http://dx.doi.org/10.1061/\(ASCE\)0733-9429\(2005\)131:12\(1074\)](http://dx.doi.org/10.1061/(ASCE)0733-9429(2005)131:12(1074)).
 25. Quecedo M, Pastor M, Herreros MI, Fernandez Merodo JA, Zhang Q. 2005. Comparison of two mathematical models for solving the dam break problem using the FEM method. *Comput.*

- Method Appl. M., 194, 3984–4005. [doi:10.1016/j.cma.2004.09.011](https://doi.org/10.1016/j.cma.2004.09.011).
26. Smagorinsky J. 1963. General circulation experiment with the primitive equations. Monthly Weather Review, 91, 99-164. [doi: http://dx.doi.org/10.1175/1520-0493\(1963\)091<0099:GCEWTP>2.3.CO;2](http://dx.doi.org/10.1175/1520-0493(1963)091<0099:GCEWTP>2.3.CO;2).
27. Xanthopoulos T, Koutitas C. 1976. Numerical simulation of two-dimensional flood wave propagation due to dam-failure. J. Hydr. Res., 14, 321–331. [doi:10.1080/00221687609499664](https://doi.org/10.1080/00221687609499664).
28. Yue W, Lin C, Patel VC. 2003. Numerical simulation of unsteady multidimensional free surface motions by level set method. Int. J. Numer. Methods Fluids, 42, 853–884. [doi:10.1002/flid.555](https://doi.org/10.1002/flid.555).

9/25/2019